Published OnlineFirst June 19, 2012; DOI:10.1158/0008-5472.CAN-11-3536

Molecular and Cellular Pathobiology

Cancer Research

Activation of Thermogenesis in Brown Adipose Tissue and Dysregulated Lipid Metabolism Associated with Cancer Cachexia in Mice

Maria Tsoli[1], Melissa Moore[1], Dominic Burg[1], Arran Painter[1], Ryland Taylor[1], Sarah H. Lockie[5], Nigel Turner[3], Alessandra Warren[2], Greg Cooney[3], Brian Oldfield[5], Stephen Clarke[4], and Graham Robertson[1]

Abstract

Cancer cachexia/anorexia is a complex syndrome that involves profound metabolic imbalances and is directly implicated as a cause of death in at least 20% to 30% of all cancers. Brown adipose tissue (BAT) plays a key role in thermogenesis and energy balance and potentially contributes to the physiologic perturbations associated with cachexia. In this study, we investigated the impact of cachexia-inducing colorectal tumor on BAT in mice. We found that brown adipocytes were smaller and exhibited profound delipidation in cachectic tumor–bearing mice. Diurnal expression profiling of key regulators of lipid accumulation and fatty acid β-oxidation and their corresponding target genes revealed dramatic molecular changes indicative of active BAT. Increased Ucp1, Pbe, and Cpt1α expression at specific points coincided with higher BAT temperatures during the dark cycle, suggestive of a temporal stimulation of thermogenesis in cachexia. These changes persisted when cachectic mice were acclimatized to 28°C confirming inappropriate stimulation of BAT despite thermoneutrality. Evidence of inflammatory signaling also was observed in the BAT as an energetically wasteful and maladaptive response to anorexia during the development of cachexia. *Cancer Res; 72(17); 4372–82. ©2012 AACR.*

Introduction

Cancer cachexia syndrome (CCS) is a progressive metabolic syndrome clinically characterized by profound weight loss, fat depletion, skeletal muscle wasting, and asthenia that are not solely attributable to inadequate nutritional intake (1). The incidence of this debilitating condition varies with tumor type, and is more common in patients with upper gastrointestinal, colorectal, and lung cancer, whereas uncommon in breast cancer. While cachexia is implicated in approximately 30% of cancer deaths, it is also responsible for reduced quality of life and increased health care costs in many other patients with cancer (2). There are currently no prognostic tests to indicate which patients with cancer are at risk of developing cachexia, and once clinical signs of cachexia are apparent, there are no effective treatments.

The molecular mechanisms that produce the profound clinical manifestations of cancer cachexia have not been elucidated. However, it is suspected that interactions between tumors and metabolic organs, in particular muscle and adipose tissue, trigger catabolic events that promote asthenia and depletion of lipid stores (3). In addition, it is unclear whether fat loss is due to cachectic mediators produced by tumors or inappropriate action of endogenous regulators in neuro/endocrine organs. Both experimental and clinical studies implicate cytokines as mediators of catabolism during cancer cachexia (4, 5), and markers of systemic inflammation have recently been incorporated into consensus clinical definitions of cachexia in multiple clinical settings including cancer (6).

Adipose tissue plays a vital role in the metabolic balance by acting as an energy reserve organ, providing stored lipids to other tissues during periods of fasting or increased metabolic demand. However, regions of BAT are not only lipid depots but can significantly contribute to energy expenditure through diet- and cold-induced thermogenesis. Activation of BAT thermogenesis is thought to be mediated by thyroid hormone and β3-adrenergic signaling pathways, which stimulate β-oxidation of fatty acids and heat production via the electron transport chain–uncoupling protein UCP1. Until recently, the physiologic function of BAT was only thought to be relevant in small mammals and infants. However, recent reports showed activated BAT in adult humans acutely exposed to cold conditions and in up to 20% patients with cancer using fludeoxyglucose positron emission tomography (^{18}F-FDG PET) scans

Authors' Affiliations: [1]Cancer Pharmacology Unit, [2]Centre for Education and Research on Ageing, ANZAC Research Institute, Concord Repatriation General Hospital, Concord; [3]Garvan Institute of Medical Research, Darlinghurst; [4]Northern Clinical School, Royal North Shore Hospital, University of Sydney, New South Wales; and [5]Department of Physiology, Monash University, Clayton, Victoria, Australia

Note: Supplementary data for this article are available at Cancer Research Online (http://cancerres.aacrjournals.org/).

M. Tsoli and M. Moore contributed equally to this work.

Corresponding Authors: Maria Tsoli, Cancer Pharmacology Unit, Anzac Research Institute, Concord Repatriation General Hospital, Hospital Road, Concord, NSW 2139, Australia. Phone: 61-2-9767-9847; Fax: 61-2-9767-9860; E-mail: mtsoli@med.usyd.edu.au; and Graham Robertson, E-mail: graham.robertson@sydney.edu.au

doi: 10.1158/0008-5472.CAN-11-3536

Published OnlineFirst June 19, 2012; DOI:10.1158/0008-5472.CAN-11-3536

(7). In addition, BAT activity correlates with body mass index with decreased BAT activation potential in obese versus lean males (8–12). While BAT has emerged as having a significant role in regulating energy balance and fat accumulation in rodents and humans, its involvement in hypermetabolic diseases such as cancer cachexia has not been extensively studied.

Energy homeostasis in metabolic organs is controlled by central and peripheral circadian clocks through tight regulation of expression and activity of enzymes involved in metabolic pathways (13). Apart from the core CLOCK-BMAL1-Reverbα–mediated transcriptional regulation, nuclear receptors have also been found to exhibit distinct diurnal expression patterns in liver, muscle, and BAT (14). Aberrant circadian rhythms result in hyperphagia, obesity, and features of the metabolic syndrome. High fat diets can also disrupt circadian rhythms and therefore further contribute to the metabolic syndrome (15, 16). Apart from the ability of melatonin, a key factor in controlling diurnal rhythms, to reduce circulating levels of TNF and IL-6 in patients with advanced cancer (17), little is known about whether circadian regulation of metabolism occurs in cancer cachexia.

In this study, we show activation of thermogenesis in BAT of cachectic mice bearing C26 tumors. The diurnal expression pattern of transcription factors and target genes involved in lipid metabolism and heat production in BAT showed distinct temporal changes that coincide with increased BAT temperature. Therefore, the development of cancer cachexia involves disruption of diurnal regulation of lipid homeostasis and thermogenesis in BAT. We also show evidence of cytokine signaling in BAT tissue implicating a role for tumor-induced systemic inflammation in modification of BAT physiology.

Materials and Methods

Cachectic Colon-26 cells were kindly provided by AMGEN. The noncachectic variant of Colon 26 was supplied by Tohuku University (Sendai, Japan). Both cell lines were grown and maintained in RPMI medium (Invitrogen) containing 10% FBS (Invitrogen) and 100 μg/mL penicillin/streptomycin (Invitrogen) in a 5% CO_2 environment.

Animal studies

Pathogen-free, 8- to 10-week-old male and BALB/c*DBA/1 (F1 hybrid), mice were purchased from Animal Resources Center (Perth, Australia) and kept at an ambient temperature of 22°C under a 12-hour light cycle (6:00 am–6:00 pm). Cachectic and noncachectic colon 26 cells were inoculated subcutaneously at 1×10^6 cells/100 μL into the right flank of mice. Control mice were similarly injected with 100 μL of RPMI medium containing antibiotics. Over a period of 14 days following inoculation, body weight, food intake, and tumor dimensions were recorded daily. Tumor-bearing and free-fed control mice had *ad libitum* access to food. One group of control mice was pair-fed to the food intake of cachectic C26–bearing group. Pair feeding was achieved by giving each pair-fed control the previous days intake of its respective C26-bearing animal. Mice were euthanized by cervical dislocation before harvesting tumors and organs, which were snap frozen in liquid nitrogen. For the thermoneutrality experiments, mice were acclimated for 5 weeks at 28°C before inoculation with either cachectic colon 26 carcinoma cells or RPMI medium. The experimental protocol was then followed as described above with the exception that the mice continued to be housed at 28°C for the duration of the experiment until harvest. All animal experimentation was carried out according to the Australian Code of Practice for the Care and Use of Animals for Scientific Purposes under the Animal Research Regulation (2005) of the New South Wales (Australia) and under a protocol approved by the Animal Welfare Committee of Sydney South-West Area Health Service.

Plasma cytokine analysis

Plasma was collected from control, pair-fed, and C26-bearing mice (cachectic and noncachectic clones) via cardiac puncture and placed in EDTA or heparin-coated sample tubes to prevent clotting. IL-6, TNFα, and INFγ levels were measured using the RnD Biosystems Quantkine Mouse IL-6, TNFα, and INFγ ELISA Kits, respectively (Bioscientific Australia).

Indirect calorimetry studies

Oxygen consumption rate (Vo_2) and respiratory exchange rate (RER) of individual mice were determined using an 8-chamber indirect calorimeter (Oxymax series; Columbus Instruments) as previously described (18).

Biotelemetry

Mice were anesthetized using 5% isoflurane in oxygen in an induction chamber and then maintained on 2% isofluorane delivered by face mask. Temperature-sensitive transmitters (E-mitters, Mini Mitter) were implanted into the interscapular BAT of the mice who had previously had intracerebroventricular cannulae implanted. Mice were shaved and a 1-cm incision was made just posterior to the scapulae to reveal the hindmost section of the white fat overlaying the interscapular area. A pocket was blunt dissected on the ventral side of the white fat to access the brown fat underneath. The E-mitter was then placed in the exposed pocket and the white fat sutured around the device. The wound was then sutured closed. After surgery, the animals received a single subcutaneous dose of 5 mg/kg meloxiocam (Metacam, Boehringer Ingelheim) in a volume of 1 mL/kg and were maintained on a heated pad until full recovery. Mice were then allowed at least 4 days of recovery before intracerebroventricular injections and recording began. Temperature and activity data were collected via receiver plate below the home cage and recorded on a PC.

Adipose tissue histology and microscopy

Brown adipose tissue samples were fixed in 10% formalin neutral-buffered solution (Sigma Aldrich), embedded in paraffin wax, and 5-μm sections cut and mounted on glass slides. After dehydration, the sections were stained with hematoxylin and eosin for histologic examination. Histology was viewed by light microscopy and examined by CAST grid software (Olympus Corp.). For electron microscopy, brown adipose fat pads were fixed in 2% glutaraldehyde in PBS for 2 hours. The fixative was then removed and tissue was rinsed with PBS.

Published OnlineFirst June 19, 2012; DOI:10.1158/0008-5472.CAN-11-3536

Fixed tissue was osmicated (1% OsO4/0.1 mol/L sodium cacodylate buffer), dehydrated in an ethanol gradient to 100%, and embedded in Spurr resin. Ultrathin sections (80-nm thick) were obtained and viewed on a Phillips CM10 transmission electron microscope.

Quantitative real-time PCR analysis

Total RNA was isolated using Trizol (Invitrogen) according to the manufacturer's protocol. First-strand cDNA was synthesized from 1 μg of total RNA using SuperScript III with random primers (Invitrogen) and oligo(dT)12-14 (Invitrogen). All primer sequences were BLASTed against the NCBI mouse genomic sequence database to ensure specificity for the corresponding gene. Primer sequences will be provided upon request. Quantitative PCR reactions contained 1.25 ng cDNA, 300 nmol/L gene-specific primers, and 12 μL SYBR Green (Invitrogen). All reactions were conducted using the Corbett Rotor Gene 6000 (Corbett Life Science). Relative mRNA levels were calculated by the comparative threshold cycle method by using *Tfrc*, *Hmbs*, and *36b4* genes as the housekeeping controls (19). The results were then expressed as fold changes of cycle threshold (C_t) value relative to controls.

Western blotting

Whole-cell extracts were obtained using Cell Lysis Buffer according to manufacturer protocol, (Cell Signaling Technologies) and were quantified by BCA Protein Acid Assay Kit (Pierce). Mitochondrial extracts were obtained as described in (20). Proteins were resolved on 10% Tris-HCl SDS-PAGE (Bio-Rad) and blotted (iBlot, Invitrogen) as described by manufacturers. Cell lysates were analyzed with the following antibodies: anti-STAT3, anti-phospho-STAT3-Ser727, and anti-uncoupling protein 1. All antibodies were obtained from Cell Signaling Technology. Densitometric analysis was conducted for Western blot analysis from 3 independent experiments using ImageJ software. Expression values of phosphorylated signals were normalized with corresponding total expression and indicated as fold change over the controls.

Statistical analysis

Data are presented as the mean ± SEM. One-way ANOVA followed by Tukey multiple comparison tests were used to assess statistical significance between groups. Differences at $P < 0.05$ were considered to be statistically significant. ANCOVA was carried out using SPSS for Mac OS X v16.0.1 (SPSS Inc.) with the final body mass as covariate and $n = 7$ mice for each group. Other calculations were carried out with Minitab statistical software.

Results

Colon-26 adenocarcinoma affects body weight, food intake, and BAT mass while maintaining energy expenditure

A significant loss of body weight (Fig. 1A), accompanied by decreased food intake and BAT mass (Fig. 1B and C), occurred 14 days after C26 tumor inoculation. In contrast, pair-fed controls experienced only a moderate reduction in body weight and BAT mass indicating that anorexia alone could not completely account for the weight change in cachectic mice (Fig. 1A and B). To differentiate the impact of cachexia from the indirect effects of reduced food intake on energy expenditure, oxygen consumption and RER were measured in C26 tumor–bearing mice, calorie-restricted, and control mice. Diurnal oxygen consumption was identical between control and cachectic animals (Supplementary Fig. S1A), whereas RER reduced to approximately 0.72 in C26 tumor–bearing animals, indicating lipids as the predominant fuel source (Supplementary Fig. S1B). The effect of food restriction on energy expenditure was examined over a shorter period of time in an effort to minimize the technical difficulties in precise food delivery to pair-fed animals housed in metabolic cages. Nontumor-bearing mice were presented with the same amount of food ingested by C26 tumor–bearing mice corresponding to days 11, 12, and 13 posttumor inoculation. A striking reduction in oxygen consumption in food-restricted animals during the entry to light cycle (Supplementary Fig. S1C) coincided with milder reduction in RER compared with cachectic mice (Supplementary Fig. S1D).

When energy expenditure/heat production was calculated as kcal/mouse over the final 3 days of C26 tumor growth or food restriction, both groups were less than the corresponding control mice (Fig 1D and E). This is likely due to the progressive reductions in body weights in cachectic and calorie-restricted mice compared with *ad lib*–fed control mice. However, when the total energy expenditure over the final 12 hours of the testing period is compared using ANCOVA with final body weight as covariate, there is a significant difference between cachectic C26 and pair-fed mice at the common body weight of 24.4 g (Fig. 1F). BAT tissue showed significant morphologic alterations in cachectic mice (Fig. 1G, iii) with apparent reductions in adipocyte size compared with free-fed and pair-fed controls (Fig. 1G, i and ii). Additional examination of BAT by transmission electron microscopy confirmed the reduction in fat droplet area in cachectic mice (Fig. 1H, ii).

Cytokine signaling in BAT of cachectic C26 tumor–bearing mice

It is widely believed that proinflammatory cytokines are crucial for the development of cancer cachexia (6). We therefore examined the levels of IL-6, TNFα, and INFγ in the plasma of C26-bearing mice. Consistent with previous studies, IL-6 concentrations were elevated in plasma from cachectic mice (Fig. 2A), whereas TNFα and INFγ were below the detection limit (data not shown). Increased expression of the IL-6 receptor and *SOCS3* genes was apparent in BAT of C26 tumor–bearing mice (Fig. 2C and D). Further evidence for cytokine signaling via the JAK/STAT pathway was shown by substantially higher phosphorylation and hence activation of STAT3 within BAT of cachectic C26 mice compared with the minor change apparent in pair-fed mice (Fig. 2D). To differentiate the effect of tumor-derived cytokines on BAT from a noncachectic cancer setting, we investigated the impact of a variant of the colon 26 tumor cell line that does not elicit cachexia. Despite the comparable growth of the noncachectic C26 tumor, plasma IL-6 levels were significantly lower, whereas

Published OnlineFirst June 19, 2012; DOI:10.1158/0008-5472.CAN-11-3536

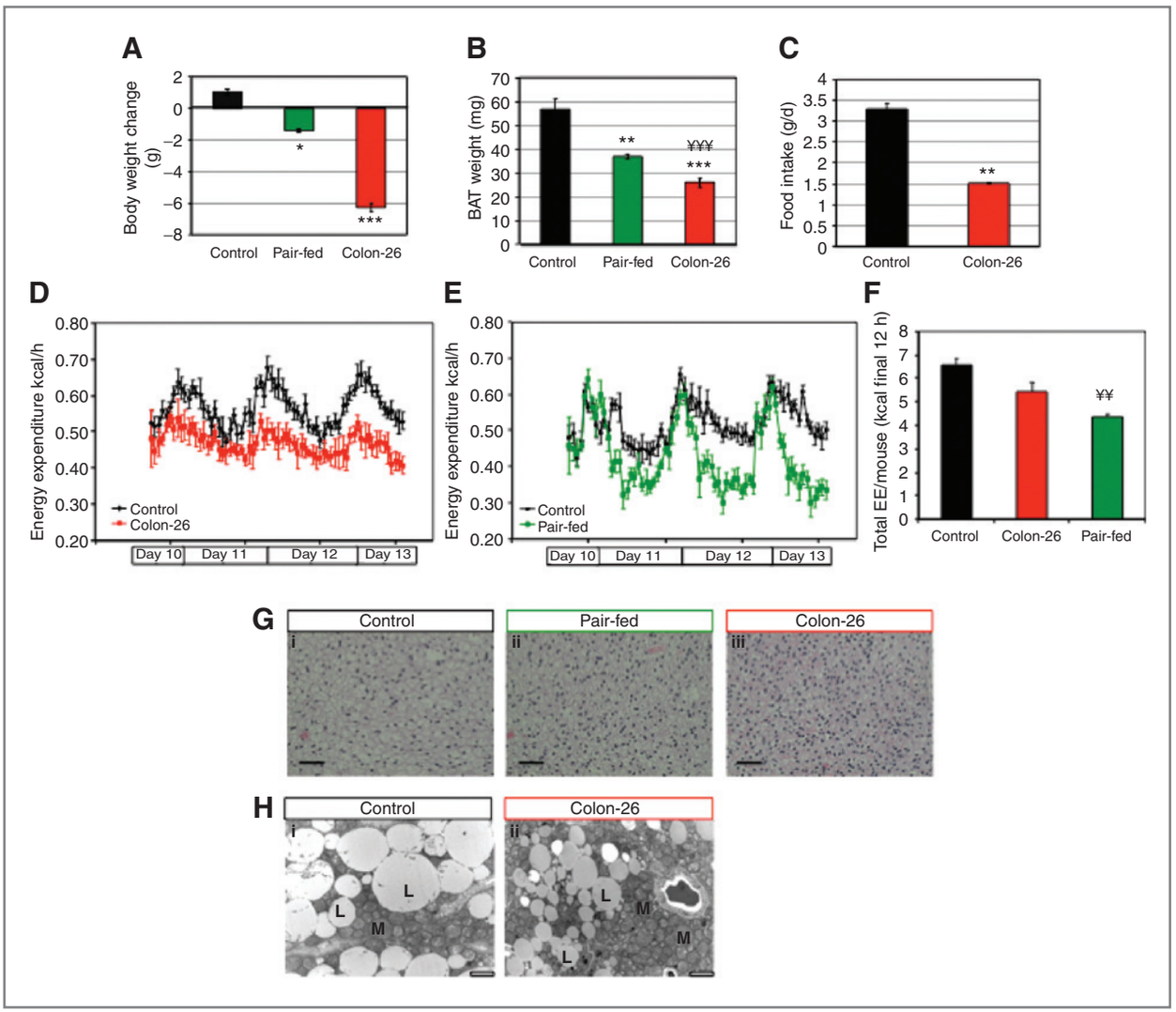

Figure 1. Metabolic parameters of mice bearing the Colon-26 tumor. A, body weight difference at day 14 (*, $P < 0.05$; ***, $P < 0.001$ vs. initial body weight). B, BAT weight changes at day 14 (**, $P < 0.01$; ***, $P < 0.01$ C26 vs. control; ¥¥¥ $P < 0.001$ C26 vs. pair-fed). C, food intake at day 14 (**, $P < 0.01$ C26 vs. control). D, energy expenditure in cachectic animals corresponding to days 11 to 13. E, energy expenditure in pair-fed mice corresponding to days 11 to 13. F, total energy expenditure during the final 12 hours of day 13 calculated by ANCOVA using final body mass as a covariate (¥¥ $P < 0.01$ C26 vs. pair-fed). G, hematoxylin and eosin staining of BAT in control free-fed (i), control pair-fed (ii), and C26 (iii) mice. Black bar represents 50 μm. H, electron microscopy images of BAT from control free-fed (i), C26 (ii) mice. Black bar represents 2 μm. L, lipid droplet; M, mitochondrion. For A, B, and C, values are presented as a mean ± SEM for 8 to 10 animals per group.

overall body, BAT weights, and mRNA expression levels of *IL6Ra* and *SOCS3* were unchanged (Fig 3.).

Perturbed diurnal expression pattern of lipid uptake and accumulation pathways in cachectic mice

To examine the impact of cancer-induced cachexia on lipid handling and *de novo* synthesis of fatty acids in brown adipocytes, we investigated the diurnal expression profile of metabolic genes and nuclear receptors at 6 time points in the light-dark cycle. Lipoprotein lipase (LPL), the major enzyme involved in hydrolysis of lipoproteins to release fatty acids for uptake into cells, normally exhibits a daily rhythm in BAT reaching its maximum peak during the dark cycle at 10:00 pm (Fig. 4A). Cachexia resulted in 4-fold higher expression as well as loss of cycling of *Lpl*. There was no significant impact of cachexia on fatty acid transporter CD36 or carrier protein AP2. In control mice, *Pparγ* and associated target genes in lipogenic and adipogenic pathways peaked during the light cycle, whereas in the tumor-bearing animals, *Pparγ*, *C/ebpα*, *Fas*, *Dgat2*, and *Perilipin* lost rhythmicity and were markedly decreased in BAT at several time points (Fig. 4B).

Altered diurnal expression of lipid utilization and thermogenesis pathways in cachectic mice

An important function of BAT is dissipation of energy in the form of heat through activation of fatty acid β-oxidation and

Published OnlineFirst June 19, 2012; DOI:10.1158/0008-5472.CAN-11-3536

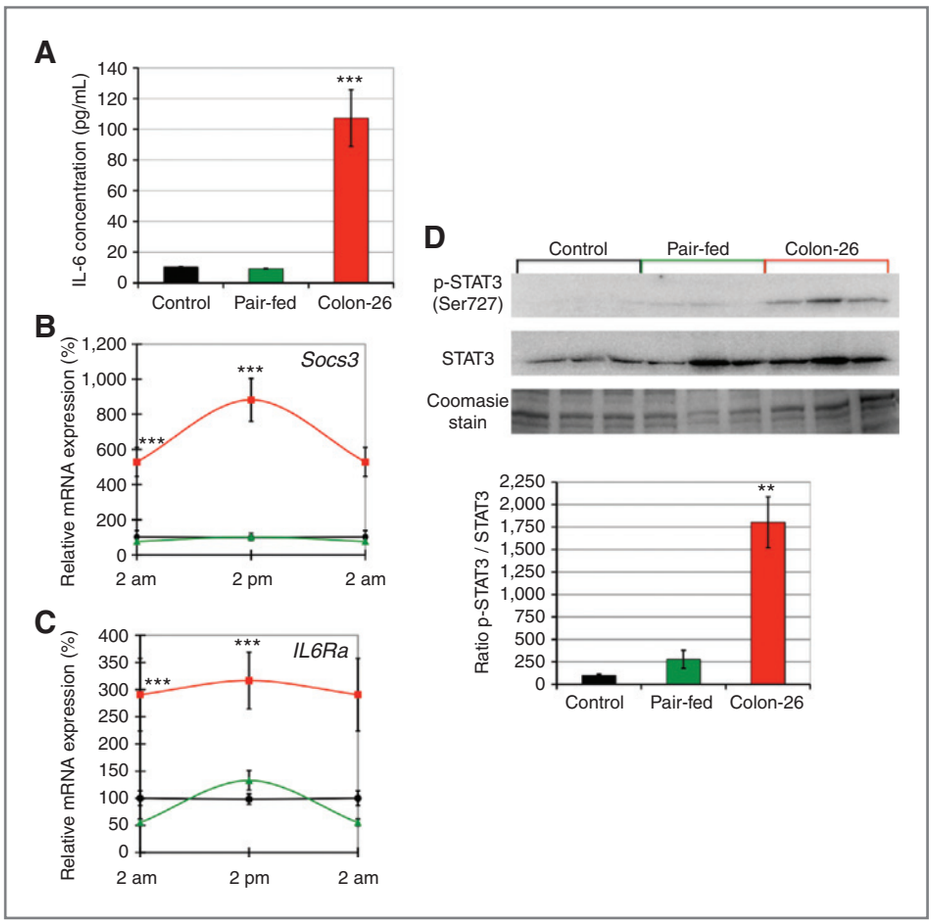

Figure 2. STAT3 signaling pathway is active in the BAT of cachectic mice but not in food-restricted mice. A, circulating IL-6 plasma levels from control, pair-fed, and C26 tumor–bearing mice (***, $P < 0.001$ C26 vs. control). B and C, mRNA analysis of *Il6Ra* and *Socs3* isolated from BAT at 2:00 am and 2:00 pm from free-fed control (black circle), pair-fed control (green triangle), and C26 tumor–bearing mice (red square; ***, $P < 0.01$ C26 vs. control). The 2:00 am values are duplicated in each graph to illustrate diurnal rhythmicity. D, protein levels of STAT3 and phosphorylated STAT3 (Ser727) in BAT of *ad lib*, pair-fed, and C26 tumor–bearing mice assessed by immunoblotting. Protein extractions were conducted in BAT harvested at 2:00 am. Values are mean ± SEM presented as percentages relative to the controls for 4 to 6 animals per group (**, $P < 0.01$ C26 vs. control).

thermogenic pathways. To understand the role of BAT in energy expenditure during cancer cachexia, we investigated the diurnal expression of transcription factors involved in regulating fatty acid catabolism and corresponding target genes (Fig. 5A). *Pparδ* normally has a diurnal oscillation peaking at 10:00 am, whereas in cachectic mice, this diurnal cycling was disrupted with higher expression at all time points. *Pgc1*, a key regulator of fatty acid metabolism, mitochondrial biogenesis, and thermogenesis maintained its diurnal peak at 10:00 am but was elevated at most time points (Fig. 5A). PPARδ target genes peroxisomal bifunctional enzyme (*PBE*) and mitochondrial carnitine palmitoyl transferase 1α (*Cpt1α*) exhibited a similar diurnal peak at early dark cycle (6:00 pm) with a 3- to 4-fold amplitude in healthy mice. BAT from cachectic mice showed higher abundance of both *Pbe* and *Cpt1α*mRNAs as well as a significant 12-hour phase advance peaking at 6:00 am. There was no change in expression of *Pbe*, *Pgc1*, and *Pparδ* in pair-fed mice (Supplementary Fig. S1).

Consistent with the previous studies (17), key mediators of the thermogenic program in BAT exhibited oscillatory patterns at specific times of the diurnal cycle (Fig. 5B). β3 adrenergic receptor (*β3AR*) transcripts peaked during the light cycle, however, in cachectic animals, this rhythm was attenuated and expression levels were reduced. Mediators of β3AR downstream signaling—adenylate cyclase 3 (*Ac3*) and deiodinase type 2 (*Dio2*)—behaved similarly at the mRNA level in healthy animals, peaking at 6:00 pm, but in cachectic mice, the rhythmic expression was disrupted and was significantly higher at all time points. In control mice, the essential mediator of heat production in BAT—*Ucp1*—displayed a diurnal pattern similar to *β3AR*. However, in cachectic mice, the *Ucp1* transcript lost its daily oscillation with maximal expression shifted towards the dark cycle. In contrast, in pair-fed mice, Ucp1 expression was reduced at 2:00 pm (Supplementary Fig. S1). These data provide compelling evidence that cachectic animals exhibited increased expression of genes involved in energy expenditure and nonshivering thermogenesis. Furthermore, the expression of genes such as *Ucp1* involved in lipolysis and thermogenesis is unaltered in BAT of mice with the noncachectic C26 tumor (Supplementary Fig. S2) that does not produce IL-6 (Fig. 3).

To determine whether these changes in gene expression coincided with heat production in cachectic animals, we assessed BAT temperature using biotelemetry devices (Fig. 5C and D). Implanted telemetry devices recorded that C26 tumor–bearing mice exhibited elevated BAT temperatures, particularly during the dark cycle, between 10 to 14 days (Fig. 5C). BAT temperature was approximately 3°C to 4°C higher in cachectic mice than in the pair-fed group. Pair fed animals had the lowest temperatures, which is in accord with the expected response to conserve energy during caloric restriction. In

Published OnlineFirst June 19, 2012; DOI:10.1158/0008-5472.CAN-11-3536

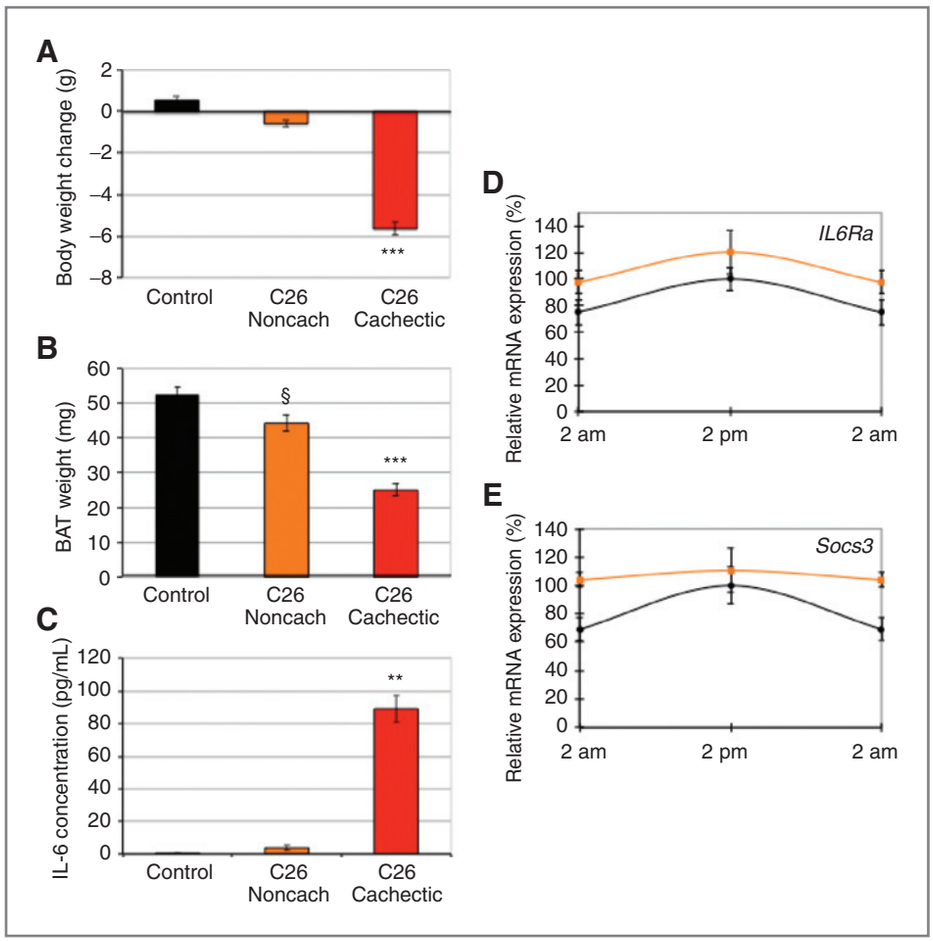

Figure 3. Metabolic parameters of mice bearing the noncachectic Colon-26 tumor and expression of genes involved in IL-6 signaling. A, body weight change between day 0 and day 14 (***, $P < 0.001$, cachectic C26 vs. control). B, BAT weight changes at day 14 (§ $P < 0.05$ noncachectic C26 vs. control; ***, $P < 0.001$ cachectic C26 vs. control). C, plasma analysis for IL-6 cytokine from control, noncachectic C26 tumor–bearing, and cachectic C26 mice (**, $P < 0.01$ cachectic C26 vs. control). D and E, mRNA analysis of *IL6Ra* and *Socs3* isolated from BAT of free-fed control (black circle) and noncachectic C26 tumor–bearing mice (orange square). The 2:00 am values are duplicated in each graph to illustrate diurnal rhythmicity. Values are mean ± SEM presented as percentages relative to the controls for 4 to 5 animals per group.

addition, physical activity appeared unchanged or even slightly reduced on days 11 to 13 in the cachectic mice indicating the source of increased temperature is unlikely to be the heat from the skeletal muscle activity (Fig. 5D). In contrast, pair-fed animals exhibited excessive physical activity despite reduced BAT temperature, likely due to foraging behavior. Therefore, activation of BAT in C26 tumor–bearing mice leads to inappropriate production of heat.

Activation of thermogenic program in BAT of cachectic mice persists at thermoneutral temperatures

To determine whether activation of BAT is due to an inability to maintain core body temperature when cachectic mice are housed under the mild cold stress of 22°C, we acclimatized the cachectic C26 mice to thermoneutral conditions—defined as a temperature (e.g., 28°C for mice) at which thermogenesis from mitochondrial electron transport chain uncoupling in BAT is not required. Similar to the previous experiments with mice housed at 22°C (Fig. 5), *β3ar* transcripts remained at lower levels in C26-bearing animals acclimated to thermoneutrality than in free- and pair-fed controls (Fig. 6). *Ucp1*, *Ac3*, and *Dio2* exhibited significantly higher levels in cachectic mice, unlike food-restricted animals. In contrast to experiments carried out at 22°C, *Ucp1* expression at 28°C was significantly higher at both 2:00 pm and 2:00 am. Other genes known to be upregulated during adaptation to cold conditions such as glycerol kinase (*GYK*) and elongation of very long chain fatty acids-like 3 (*Elovl3*) were also increased in cachectic mice at 28°C.

We assessed UCP1 protein abundance to determine whether the cumulative, temporal-specific increments in Ucp1 mRNA in BAT, during the development of cachexia, results in a net increase of UCP1 protein. Mitochondrial protein preparations of BAT from cachectic animals contained significantly more UCP1 protein compared with controls, whereas pair-fed mice had decreased mitochondrial UCP1 protein (Fig. 6B and C). Interestingly, the total mitochondrial protein yield per BAT in pair-fed mice was significantly reduced relative to control mice (Fig. 6D), presumably as part of the normal response to conserve energy by dampening BAT activity when calorie intake is chronically restricted. Therefore, when total UCP1 protein content is expressed per BAT organ (Fig. 6E), the increase exhibited by cachectic C26 tumor–bearing mice is even more striking when compared with pair-fed mice.

Discussion

The importance of weight loss in cancer has been recognized for many years and has been generally attributed to muscle

Published OnlineFirst June 19, 2012; DOI:10.1158/0008-5472.CAN-11-3536

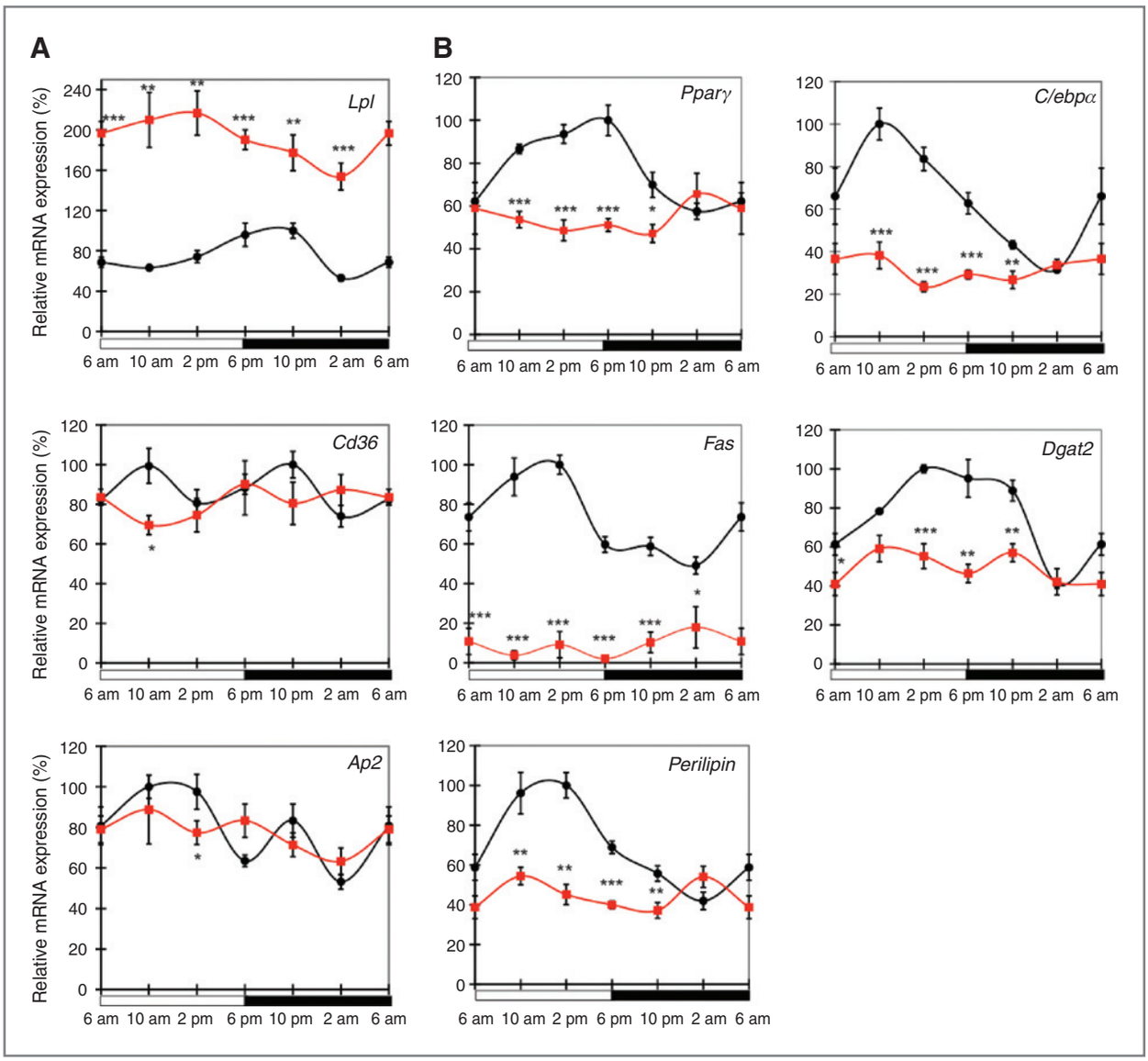

Figure 4. Expression of genes involved in lipid uptake, trafficking, and accumulation. The mRNA analysis of *Lpl*, *Cd36*, *Ap2*, *Pparγ*, *C/ebpα*, *Fas*, *Dgat2*, *and Perilipin* isolated from BAT of free-fed control (black circle) and C26-bearing mice (red square). The 6:00 am values are duplicated in each graph to illustrate a complete 24-hour cycle. Values are mean ± SEM presented as percentages relative to the controls for 4 to 5 animals per group. (*, $P < 0.05$; **, $P < 0.01$; ***, $P < 0.001$ C26 vs. control).

wasting and fat depletion (21). Earlier studies investigated limited molecular features of BAT in tumor-bearing or cytokine-administered animals (22–27). However, no systematic evaluation of lipid regulatory and metabolic genes in BAT, combined with energy expenditure and temperature assessment, has been conducted in mice that exhibit sufficient features of cancer cachexia to satisfy the consensus clinical definition (6). Furthermore, diurnal regulation of thermogenesis in BAT has not been considered in cancer or other disease settings. We show, for the first time, thermogenic activation of BAT in cachectic animals that cannot be attributed to the effects of reduced food intake or inability to maintain core body temperature.

Because anorexia is associated with cachexia in patients with cancer, we assessed changes in pair-fed animals presented with the same progressive food reduction as cachectic mice. The profound delipidation of BAT and increased expression of molecular regulators of lipid metabolism and target genes were not evident in pair-fed mice (Fig. 6 and Supplementary Fig. S2). Indeed, UCP1, the hallmark of thermogenic activation in BAT, was reduced at both mRNA and protein levels in response to food restriction while being increased in cachexia (Fig. 6). The observation that anorectic C26 cachectic mice maintain whole body energy expenditure at a higher level than corresponding sized calorie-restricted mice (Fig. 1F and Supplementary Fig. S1) while showing increased BAT and body surface

Published OnlineFirst June 19, 2012; DOI:10.1158/0008-5472.CAN-11-3536

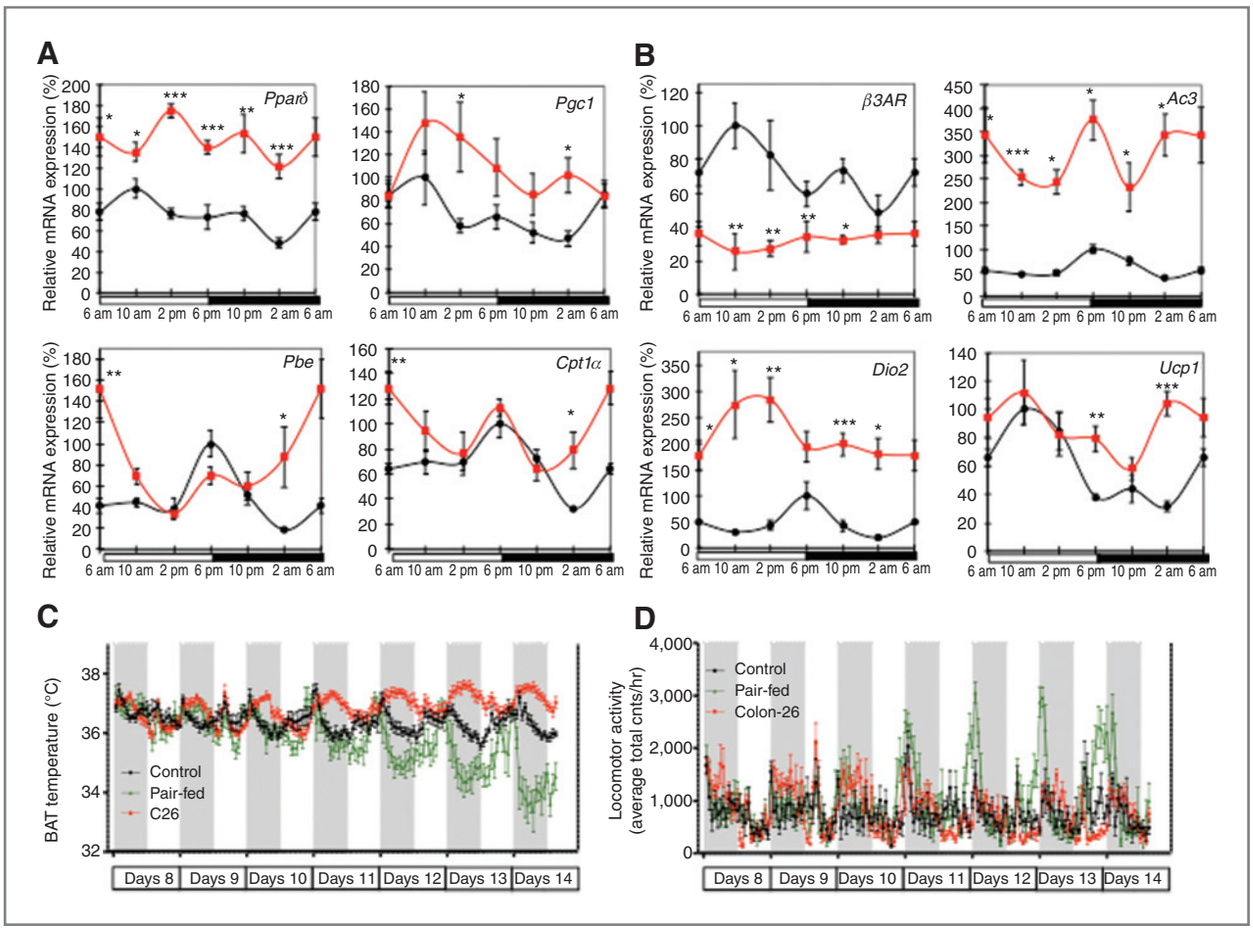

Figure 5. Expression of genes involved in lipolysis and activation of thermogenesis in BAT. A and B, mRNA analysis of *Pparγ*, *Pgc1*, *Pbe*, *Cpt1a*, *b3AR*, *Ac3*, *Dio2*, and *Ucp1* isolated from BAT of free-fed control (black circle) and C26-bearing mice (red square). Values are mean ± SEM presented as percentages relative to the controls for 4 to 5 animals per group (*, $P < 0.05$; **$P < 0.01$; ***, $P < 0.001$ C26 vs. control). The 6:00 am values are duplicated in each graph to illustrate a complete 24-hour cycle. C and D, changes in BAT temperatures and locomotor activity measured by implanted biotelemetry devices. Data represent the group means of the temperature and physical activity for each animal at each time point for the final 7 days. C26-bearing mice (red), free-fed control (black), and pair-fed control (green).

temperatures provides further evidence of energetically wasteful processes in cachectic animals. This directly contrasts the effort to conserve energy in response to reduced calorie intake observed in pair-fed mice (Figs. 1 and 5). This apparent maladaptive response to caloric restriction in cachexia could have clinical relevance, as hypermetabolism is prominent in certain cancers such as lung, pancreatic, and leukemia (28, 29). The changes in the diurnal pattern of gene expression in BAT of cachectic mice are striking, especially the increases in *Pbe*, *Cpt1α*, and *Ucp1* that coincide with elevated BAT temperatures during the dark cycle when heat generation from increased physical activity would normally diminish the requirement for BAT-mediated thermogenesis. To our knowledge, this is the first demonstration of altered diurnal expression of genes involved in lipid metabolism and thermogenesis linked to diurnal increases in BAT temperature due to cancer. Most of the genes examined in this study normally exhibit a diurnal rhythm, peaking either during the light cycle or at entry to the dark cycle (14). A recent study by Zvonic and colleagues (30) found that approximately 5,000 genes rhythmically expressed in BAT indicate synchronization of diurnal functions with physiologic processes mediated primarily by circadian clock regulators and nuclear receptors (16). C26 tumor–bearing mice exhibited disrupted diurnal rhythmicity and phase shifting in BAT indicative of diminished *de novo* synthesis and storage of lipids (*Pparγ*, *C/ebpα*, *Fas*, *Dgat2*, and *Perilipin*), increased uptake of lipids for β-oxidation rather than storage (*Lpl*), and energy expenditure (*Pparδ*). It will be interesting to explore the interplay of cytokine and neuro-endocrine signals responsible for the temporal coupling of increased BAT temperatures with upregulated *Ucp1*, *Pbe*, and *Cpt1α* expression alongside the uniform changes in thermogenic regulators *Pgc1α*, *Ac3*, *β3ar*, and *Dio2*.

Our initial findings of activation of BAT in cachexia were derived from experiments with tumor-bearing mice housed at 22°C, a temperature that elicits mild chronic cold stress. Therefore, it is possible that this response may be due to an inability of cachectic mice to maintain core body temperature,

Published OnlineFirst June 19, 2012; DOI:10.1158/0008-5472.CAN-11-3536

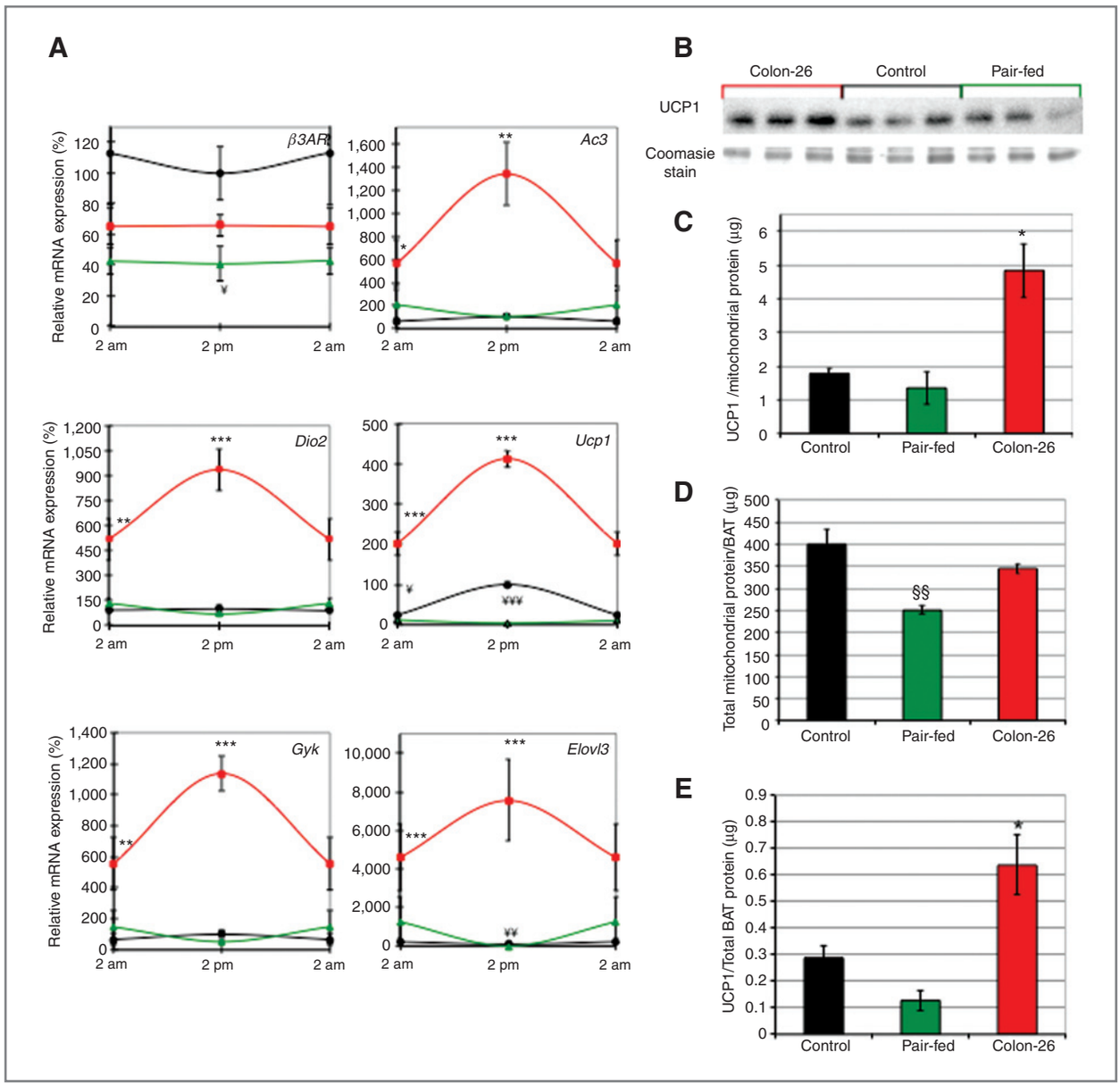

Figure 6. Expression of cold-adaptive genes and increased protein levels of UCP1 in BAT under conditions of thermoneutrality. A, mRNA analysis of *B3Ar*, *Ac3*, *Dio2*, *Ucp1*, *Gyk*, and *Elovl3* isolated from BAT of free-fed control (black circle), pair-fed control (green triangle), and C26-bearing mice (red square). The 2:00 am values are duplicated in each graph to illustrate diurnal rhythmicity. B and C, relative protein concentration of UCP1 in mitochondria isolated from cachectic, control, and pair-fed animals. D, total mitochondrial protein content in C26-bearing, control, and pair-fed mice. E, protein levels of UCP1 expressed per total mitochondrial protein content in BAT from cachectic, control, and pair-fed animals. Values are mean ± SEM presented as percentages relative to the controls for 4 to 5 animals per group (*, $P < 0.05$; **, $P < 0.01$; ***, $P < 0.001$ C26 vs. control; ¥ $P < 0.05$; ¥¥ $P < 0.01$; ¥¥¥ $P < 0.001$ C26 vs. pair-fed; §§ $P <$ pair-fed vs. control).

as observed in hypothermic MAC16 tumor–bearing mice that had increased UCP1 (31). To distinguish whether the observed changes in BAT are due to such a compensatory adaptation or a more active signal emanating directly from the tumor, we housed the cachectic C26 mice under thermoneutral conditions, defined as a temperature (e.g., 28–30°C for mice) at which obligatory heat dissipation is sufficient to defend normothermic body temperature without thermoregulatory heat production. The changes in cachectic mice persisted at thermoneutrality (Fig. 6) and were even greater than those apparent at 22°C relative to both control and pair-fed mice. Furthermore, expression of 2 genes associated with BAT hypertrophy during cold conditions (32), *Elovl3* and *Gyk* were also increased. The value of conducting such investigations of complex metabolic syndromes involving energy imbalance at thermoneutrality is reinforced by recent studies with Ucp1 knockout mice that defined a role for UCP1 in diet-induced thermogenesis (33). This finding had eluded previous attempts

Published OnlineFirst June 19, 2012; DOI:10.1158/0008-5472.CAN-11-3536

at uncovering a phenotype for UCP1 when mice were acclimated to normal animal housing temperatures (34).

While the type of tumor, stage, and duration of disease can influence resting energy expenditure, the systemic inflammatory status may also play an important role as high levels of cytokines and acute phase proteins have been observed in hypermetabolic patients with lung and pancreatic cancer (35, 36). Because cytokines are considered etiologic factors of cancer-induced energy wastage, as well as part of the consensus clinical definition of cachexia (5, 6), we investigated their potential involvement in the C26 model and observed plasma IL-6 levels within the range reported in patients with cancer. IL-6 may enhance thermogenesis via direct action on BAT or by sympathetic nervous system (SNS) stimulation. For example, ventricular administration or hypothalamic expression of IL-6 increased energy expenditure, lipolysis, and UCP1 expression via the SNS (37, 38). However, IL-6 induced fat-burning can also be exerted by an SNS-independent mechanism such as AMPK activation (39). Another pathway by which IL-6 could mediate direct effects on BAT is via MAP kinases. In response to SNS stimulation, catecholamines signal through β-adrenergic receptors to enhance thermogenesis in BAT by activating p38 MAPK, thereby increasing mitochondrial biogenesis, expression of Pgc1α and Ucp1, and uncoupling (40, 41). The recent demonstration of a parallel pathway involving systemic cardiac–derived natriuretic peptides, cGMP and protein kinase B that also operate via p38 (42) further highlights the importance of MAPKs in BAT thermogenic regulation. As IL-6 is a potent activator of MAPKs via Ras/raf, it may bypass the β-adrenergic and natriuretic protein receptors and their downstream effectors cAMP/PKA and cGMP/PKG to upregulate UCP1. Increased UCP1 mRNA and protein abundance may augment net UCP1 uncoupling activity promoted by elevated fatty acid availability in brown adipocytes due to enhanced lipolysis.

While the effects of IL-6 through the SNS have not been investigated in the present study, our work supports the concept of cytokine-driven hypermetabolism and fat depletion in the cachectic animals. The exploration of the differences between cachectogenic and noncachectogenic variants of the colon 26 tumor provides further intriguing evidence of cytokine involvement in BAT activation. This is evident in the failure of the noncachectogenic, C26 variant to affect BAT (Fig. 3 and Supplementary Fig. S3) coupled with a lack of corresponding circulating cytokines. Further studies into IL-6 or other cytokine signaling cascades operative in BAT of cachectic animals are required to define the links between tumor-derived cytokines and enhanced thermogenesis in cancer.

Clinical studies have found an association between cancer cachexia, systemic cytokines, and fever (43). In particular, leukemia/lymphoma patients with B-symptoms (night sweats, weight loss, and fever >38°C) have elevated C-reactive protein (CRP) together with reduced survival compared with patients without B-symptoms (44). These issues also occur in pediatric malignancies where there is greater concern due to the limited energy reserves and higher nutrient requirements in children (45). Despite the longstanding awareness of BAT in newborns and recent confirmation in adults through ^{18}FDG PET imaging (8, 10, 11), there is no information about the association of active brown fat, plasma cytokines, or CRP levels and weight loss in cancer patients. An early study found the morphologic evidence of BAT in the peri-renal fat pad from 80% of cancer patients with cachexia (46). In view of the high prevalence of functionally active BAT in patients with cancer, which approached 20% after serial PET scans (7), it will be interesting to correlate weight loss and inflammatory markers with activated BAT in sequential PET scans. Nevertheless, we cannot rule out the impact of other unidentified, yet tumor-derived factors or the involvement of SNS system on BAT activation.

In conclusion, based on these studies in a clinically relevant murine model of cachexia, reduced food intake is not the sole mechanism leading to weight loss during the development of cachexia. Rather, dysregulated diurnal expression of transcription factors that control lipid metabolism and thermogenesis in BAT are likely to contribute to the fat depletion, elevated temperatures, and hypermetabolic state of cancer cachexia.

Disclosure of Potential Conflicts of Interest

No potential conflicts of interest were disclosed.

Authors' Contributions

Conception and design: M. Tsoli, M. Moore, S. Clarke, G. Robertson
Development of methodology: M. Tsoli, M. Moore, A. Painter, B. Oldfield, S. Clarke, G. Robertson
Acquisition of data (provided animals, acquired and managed patients, provided facilities, etc.): M. Tsoli, M. Moore, D. Burg, A. Painter, R. Taylor, S.H. Lockie, N. Turner, A. Warren, G. Cooney, S. Clarke, G. Robertson
Analysis and interpretation of data (e.g., statistical analysis, biostatistics, computational analysis): M. Tsoli, M. Moore, D. Burg, A. Painter, S.H. Lockie, N. Turner, G. Cooney, S. Clarke, G. Robertson
Writing, review, and/or revision of the manuscript: M. Tsoli, M. Moore, M. Moore, D. Burg, A. Painter, N. Turner, G. Cooney, B. Oldfield, S. Clarke, G. Robertson
Administrative, technical, or material support (i.e., reporting or organizing data, constructing databases): M. Moore, A. Painter, B. Oldfield, S. Clarke
Study supervision: M. Tsoli, S. Clarke, G. Robertson

Acknowledgments

The authors thank the MPU facility at the ANZAC Research Institute for their technical support, the Garvan Institute and Monash University Animal Services and AMGEN for supplying the C26 tumor cells. The authors also thank Drs. Glen Reid and Noeris Salam for reading this manuscript and Dr. Erdahl Teber for advice on statistics.

Grant Support

This work was funded by the SCRIPT Cancer Institute NSW Translational Program Grant for Colorectal Cancer (#06/TPG/1-02).

The costs of publication of this article were defrayed in part by the payment of page charges. This article must therefore be hereby marked *advertisement* in accordance with 18 U.S.C. Section 1734 solely to indicate this fact.

Received October 28, 2011; revised June 1, 2012; accepted June 5, 2012; published OnlineFirst June 19, 2012.

References

1. Bruera E. ABC of palliative care. Anorexia, cachexia, and nutrition. BMJ 1997;315:1219–22.
2. Palesty JA, Dudrick SJ. What we have learned about cachexia in gastrointestinal cancer. Dig Dis 2003;21:198–213.

Published OnlineFirst June 19, 2012; DOI:10.1158/0008-5472.CAN-11-3536

3. Skipworth RJE, Stewart GD, Dejong CHC, Preston T, Fearon KCH. Pathophysiology of cancer cachexia: much more than host-tumour interaction? Clin Nutr 2007;26:667–76.
4. Bennani-Baiti N, Davis MP. Cytokines and cancer anorexia cachexia syndrome. Am J Hosp Palliat Care 2008;25:407–11.
5. Carson JA, Baltgalvis KA. Interleukin 6 as a key regulator of muscle mass during cachexia. Exerc Sport Sci Rev 2010;38:168–76.
6. Evans WJ, Morley JE, Argilés J, Bales C, Baracos V, Guttridge D, et al. Cachexia: a new definition. Clin Nutr 2008;27:793–9.
7. Lee P, Greenfield JR, Ho KKY, Fulham MJ. A critical appraisal of the prevalence and metabolic significance of brown adipose tissue in adult humans. Am J Physiol Endocrinol Metab 2010;299:E601–6.
8. Cypess AM, Lehman S, Williams G, Tal I, Rodman D, Goldfine AB, et al. Identification and importance of brown adipose tissue in adult humans. N Engl J Med 2009;360:1509–17.
9. Nedergaard J, Bengtsson T, Cannon B. Unexpected evidence for active brown adipose tissue in adult humans. Am J Physiol Endocrinol Metab 2007;293:E444–52.
10. van Marken Lichtenbelt WD, Vanhommerig JW, Smulders NM, Drossaerts JMAFL, Kemerink GJ, Bouvy ND, et al. Cold-activated brown adipose tissue in healthy men. N Engl J Med 2009;360:1500–8.
11. Virtanen KA, Lidell ME, Orava J, Heglind M, Westergren R, Niemi T, et al. Functional brown adipose tissue in healthy adults. N Engl J Med 2009;360:1518–25.
12. Yoneshiro T, Aita S, Matsushita M, Kameya T, Nakada K, Kawai Y, et al. Brown adipose tissue, whole-body energy expenditure, and thermogenesis in healthy adult men. Obesity 2011:19:13–6.
13. Maury E, Ramsey KM, Bass J. Circadian rhythms and metabolic syndrome: from experimental genetics to human disease. Circ Res 2010;106:447–62.
14. Yang X, Downes M, Yu RT, Bookout AL, He W, Straume M, et al. Nuclear receptor expression links the circadian clock to metabolism. Cell 2006;126:801–10.
15. Kennaway DJ, Owens JA, Voultsios A, Boden MJ, Varcoe TJ. Metabolic homeostasis in mice with disrupted Clock gene expression in peripheral tissues. Am J Physiol Regul Integr Comp Physiol 2007;293:R1528–R37.
16. Kohsaka A, Laposky AD, Ramsey KM, Estrada C, Joshu C, Kobayashi Y, et al. High-fat diet disrupts behavioral and molecular circadian rhythms in mice. Cell Metab 2007;6:414–21.
17. Mahmoud F, Sarhill N, Mazurczak MA. The therapeutic application of melatonin in supportive care and palliative medicine. Am J Hosp Palliat Care 2005;22:295–309.
18. Turner N, Bruce CR, Beale SM, Hoehn KL, So T, Rolph MS, et al. Excess lipid availability increases mitochondrial fatty acid oxidative capacity in muscle: evidence against a role for reduced fatty acid oxidation in lipid-induced insulin resistance in rodents. Diabetes 2007;56:2085–92.
19. Vandesompele J, De Preter K, Pattyn F, Poppe B, Van Roy N, De Paepe A, et al. Accurate normalization of real-time quantitative RT-PCR data by geometric averaging of multiple internal control genes. Genome Biol 2002;3:RESEARCH0034.
20. Cannon B, Lindberg O. Mitochondria from brown adipose tissue: isolation and properties. Methods Enzymol 1979;55:65–78.
21. Fearon KCH. Cancer cachexia: developing multimodal therapy for a multidimensional problem. Eur J Cancer 2008;44:1124–32.
22. Arruda AP, Milanski M, Romanatto T, Solon C, Coope A, Alberici LC, et al. Hypothalamic actions of tumor necrosis factor provide the thermogenic core for the wastage syndrome in cachexia. Endocrinology 2010;151:683–94.
23. Bing C, Russell S, Becket E, Pope M, Tisdale MJ, Trayhurn P, et al. Adipose atrophy in cancer cachexia: morphologic and molecular analysis of adipose tissue in tumour-bearing mice. Br J Cancer 2006;95:1028–37.
24. Roe S, Cooper AL, Morris ID, Rothwell NJ. Mechanisms of cachexia induced by T-cell leukemia in the rat. Metab Clin Exp 1996;45:645–51.
25. Brooks SL, Neville AM, Rothwell NJ, Stock MJ, Wilson S. Sympathetic activation of brown-adipose-tissue thermogenesis in cachexia. Biosci Rep 1981;1:509–17.
26. Oudart H, Calgari C, Andriamampandry M, Le Maho Y, Malan A. Stimulation of brown adipose tissue activity in tumor-bearing rats. Can J Physiol Pharmacol 1995;73:1625–31.
27. Edström S, Kindblom LG, Lindmark L, Lundholm K. Metabolic and morphologic changes in brown adipose tissue from non-growing mice with an isogeneic sarcoma. Evaluation with respect to development of cachexia. Int J Cancer; 1986;37:753–60.
28. Cao D-X, Wu G-H, Zhang B, Quan Y-J, Wei J, Jin H, et al. Resting energy expenditure and body composition in patients with newly detected cancer. Clin Nutr 2010;29:72–7.
29. Lerebours E, Tilly H, Rimbert A, Delarue J, Piguet H, Colin R. Change in energy and protein status during chemotherapy in patients with acute leukemia. Cancer 1988;61:2412–7.
30. Zvonic S, Ptitsyn AA, Conrad SA, Scott LK, Floyd ZE, Kilroy G, et al. Characterization of peripheral circadian clocks in adipose tissues. Diabetes 2006;55:962–70.
31. Bing C, Brown M, King P, Collins P, Tisdale MJ, Williams G. Increased gene expression of brown fat uncoupling protein (UCP)1 and skeletal muscle UCP2 and UCP3 in MAC16-induced cancer cachexia. Cancer Res 2000;60:2405–10.
32. Watanabe M, Yamamoto T, Mori C, Okada N, Yamazaki N, Kajimoto K, et al. Cold-induced changes in gene expression in brown adipose tissue: implications for the activation of thermogenesis. Biol Pharm Bull 2008;31:775–84.
33. Feldmann HM, Golozoubova V, Cannon B, Nedergaard J. UCP1 ablation induces obesity and abolishes diet-induced thermogenesis in mice exempt from thermal stress by living at thermoneutrality. Cell Metab 2009;9:203–9.
34. Cannon B, Nedergaard J. Nonshivering thermogenesis and its adequate measurement in metabolic studies. J Exp Biol 2011;214:242–53.
35. Falconer JS, Fearon KC, Plester CE, Ross JA, Carter DC. Cytokines, the acute-phase response, and resting energy expenditure in cachectic patients with pancreatic cancer. Ann Surg 1994;219:325–31.
36. Simons JP, Schols AM, Buurman WA, Wouters EF. Weight loss and low body cell mass in males with lung cancer: relationship with systemic inflammation, acute-phase response, resting energy expenditure, and catabolic and anabolic hormones. Clin Sci 1999;97:215–23.
37. Li G, Klein RL, Matheny M, King MA, Meyer EM, Scarpace PJ. Induction of uncoupling protein 1 by central interleukin-6 gene delivery is dependent on sympathetic innervation of brown adipose tissue and underlies one mechanism of body weight reduction in rats. Neuroscience 2002;115:879–89.
38. Wallenius K, Wallenius V, Sunter D, Dickson SL, Jansson JO. Intracerebroventricular interleukin-6 treatment decreases body fat in rats. Biochem Biophys Res Commun 2002;293:560–5.
39. Kelly M, Keller C, Avilucea PR, Keller P, Luo Z, Xiang X, et al. AMPK activity is diminished in tissues of IL-6 knockout mice: the effect of exercise. Biochem Biophys Res Commun 2004;23:449–54.
40. Cao W, Daniel KW, Robidoux J, Puigserver P, Medvedev AV, Bai X, et al. P38 mitogen-activated protein kinase is the central regulator of cyclic AMP-dependent transcription of the brown fat uncoupling protein 1 gene. Mol Cell Biol 2004;24:3057–67.
41. Collins S, Yehuda-Shnaidman E, Wang H. Positive and negative control of Ucp1 gene transcription and the role of beta-adrenergic signalling networks. Int J Obes 2010;34:S28–S33.
42. Bordicchia M, Liu D, Amri EZ, Ailhaud G, Dessì-Fulgheri P, Zhang C, et al. Cardiac natriuretic peptides act via p38 MAPK to induce the brown fat thermogenic program in mouse and human adipocytes. J Clin Invest 2012;122:1022–36.
43. Kurzrock R. The role of cytokines in cancer-related fatigue. Cancer 2001;92:1684–8.
44. Sharma R, Cunningham D, Smith P, Robertson G, Dent O, Clarke SJ. Inflammatory (B) symptoms are independent predictors of myelosuppression from chemotherapy in Non-Hodgkin Lymphoma (NHL) patients–analysis of data from a British National Lymphoma Investigation phase III trial comparing CHOP to PMitCEBO. BMC Cancer 2009;9:153.
45. Andrassy RJ, Chwals WJ. Nutritional support of the pediatric oncology patient. Nutrition 1998;14:124–9.
46. Shellock F, Riedinger M, Fishbein M. Brown adipose tissue in cancer patients: possible cause of cancer-induced cachexia. J Cancer Res Clin Oncol 1986;111:82–5.

Published OnlineFirst June 19, 2012; DOI:10.1158/0008-5472.CAN-11-3536

Cancer Research

Activation of Thermogenesis in Brown Adipose Tissue and Dysregulated Lipid Metabolism Associated with Cancer Cachexia in Mice

Maria Tsoli, Melissa Moore, Dominic Burg, et al.

Cancer Res 2012;72:4372-4382. Published OnlineFirst June 19, 2012.